



**HAL**  
open science

# Influence of EGR and Syngas Components on the Autoignition of Natural Gas in a Rapid Compression Machine: A Detailed Experimental Study

Y. Yu, G. Vanhove, J. Griffiths, S. de Ferrières, J.-F. Pauwels

► **To cite this version:**

Y. Yu, G. Vanhove, J. Griffiths, S. de Ferrières, J.-F. Pauwels. Influence of EGR and Syngas Components on the Autoignition of Natural Gas in a Rapid Compression Machine: A Detailed Experimental Study. *Energy & Fuels*, 2013, 27 (7), pp.3988 - 3996. 10.1021/ef400336x . hal-01738389

**HAL Id: hal-01738389**

**<https://hal.science/hal-01738389>**

Submitted on 14 Sep 2020

**HAL** is a multi-disciplinary open access archive for the deposit and dissemination of scientific research documents, whether they are published or not. The documents may come from teaching and research institutions in France or abroad, or from public or private research centers.

L'archive ouverte pluridisciplinaire **HAL**, est destinée au dépôt et à la diffusion de documents scientifiques de niveau recherche, publiés ou non, émanant des établissements d'enseignement et de recherche français ou étrangers, des laboratoires publics ou privés.

**Influence of EGR components on the autoignition of natural gas in a rapid compression machine: a detailed experimental study**

|                               |  |
|-------------------------------|--|
| Journal:                      | <i>Energy &amp; Fuels</i>  |
| Manuscript ID:                | Draft  |
| Manuscript Type:              | Article  |
| Date Submitted by the Author: | n/a  |
| Complete List of Authors:     | Yu, Yi; PC2A - UMR 5822 CNRS/Lille 1, Vanhove, Guillaume; PC2A - UMR 5822 CNRS/Lille 1, Griffiths, John; School of Chemistry, De Ferrières, Solène; CRIGEN - Centre de Recherche et Innovation en Gaz et Energies Nouvelles, Pauwels, Jean-François; PC2A - UMR 5822 CNRS/Lille 1, |
|                               |  |

SCHOLARONE™  
Manuscripts

1  
2  
3 **Influence of EGR components on the autoignition of natural gas in a**  
4  
5 **rapid compression machine: a detailed experimental study**  
6  
7

8  
9  
10 Y. Yu<sup>1</sup>, G. Vanhove<sup>1\*</sup>, J.F. Griffiths<sup>2</sup>, S. De Ferrières<sup>3</sup>, J.-F. Pauwels<sup>1</sup>  
11

12 <sup>1</sup> PC2A - UMR 5822 CNRS/Lille 1. Université Lille1 Sciences et Technologies, Cité  
13  
14 scientifique, 59655 Villeneuve d'Ascq Cedex, France  
15

16 <sup>2</sup> School of Chemistry, The University, Leeds, LS2 9JT, United Kingdom.  
17

18 <sup>3</sup> CRIGEN - Centre de Recherche et Innovation en Gaz et Energies Nouvelles, GDF  
19  
20 SUEZ, 361 Avenue du Président Wilson, 93210 St Denis la Plaine, France  
21  
22  
23  
24  
25  
26  
27  
28  
29  
30  
31  
32  
33  
34  
35  
36  
37  
38  
39  
40  
41  
42

43 \*: Corresponding author  
44 Guillaume Vanhove  
45 PC2A – UMR 8522 CNRS/Lille 1  
46 Université de Lille 1 – Sciences et Technologies  
47 Cité scientifique  
48 59655 Villeneuve d'ascq CEDEX  
49 France  
50 Tel: +333.20.43.44.85  
51 Fax: +333.20.43.69.77  
52 e-mail: [guillaume.vanhove@univ-lille1.fr](mailto:guillaume.vanhove@univ-lille1.fr)  
53  
54  
55  
56  
57  
58  
59  
60

**Abstract**

A detailed experimental study was performed in a rapid compression machine to investigate the effect of several EGR components on the autoignition of natural gas. Ignition delays of methane, natural gas and mixtures of natural gas with hydrogen, carbon monoxide, carbon dioxide and water were measured for temperatures ranging from 870 K to 1000 K and pressures from 18 to 24 bar, at equivalence ratios 1 and 0.7. The results show an accelerating effect of H<sub>2</sub> blending. The experimental measurements are compared with results from numerical simulations using detailed chemical mechanisms from the literature. Natural gas ignition delays can be reproduced satisfactorily, but improvements need to be made to give an accurate, quantitative account of the effect of the inclusion hydrogen.

**Keywords:** RCM, natural gas, ignition, EGR, hydrogen.

## 1. Introduction

Natural gas (NG) is widely recognised as a very convenient automotive fuel: its high H/C ratio involves lower CO<sub>2</sub> emissions than conventional fuels; it has high combustion efficiency, it induces lower CO and unburned hydrocarbons emissions and has a low propensity to knock [1]. It is readily available as a fossil resource, but can also be synthesised from biomass [2-4]. As a consequence, surrogate compositions of NG, have been widely studied in combustion systems, including burners [5], rapid compression machines [6-9] and shock tubes [10, 11]. Investigations prior to 1994 were reviewed by Spadaccini and Colkett [12]. It is well understood that the reactivity of natural gas is correlated to its content of higher hydrocarbons, such as ethane and propane, especially in the low and intermediate temperature regime [7, 8, 13-16].

However, the use of EGR technology in modern engines, as well as the eventual presence of impurities in synthesised NG, indicates a need for detailed studies on the effect of additional components on the ignition delays of NG in engine conditions. The present study relates to the inclusion of H<sub>2</sub>, CO, CO<sub>2</sub> and H<sub>2</sub>O individually in mixtures with natural gas and the experimental investigation of the subsequent variation of ignition delay following compression in a rapid compression machine (RCM) to temperatures in the range 880 - 960 K and pressures in the range 18 - 22 bar.

The addition of hydrogen to gaseous fuels has the advantage of reducing CO<sub>2</sub> emissions when hydrogen is obtained from non-fossil resources. However, this addition can have an effect on the knock propensity of the fuel in spark ignition engines, which also needs to be addressed [17]. Carbon monoxide also has some

1  
2  
3 part to play as a reactive, heat generating component but carbon dioxide and water  
4  
5 have largely inert roles, apart from the potential for limited, kinetic contributions or  
6  
7 through their enhanced heat capacity relative to that of monatomic or diatomic  
8  
9 molecules.

10  
11 The purpose of the present investigation is to provide experimental data to elucidate  
12  
13 how these supplementary components affect the autoignition of a typical NG  
14  
15 composition. Experimental comparisons are also made between the combustion of  
16  
17 NG and pure CH<sub>4</sub>. In addition, with the distinctions between NG and pure CH<sub>4</sub> in  
18  
19 mind, in order to guide further developments that may be necessary for the  
20  
21 application of numerical investigations to the influence of EGR components on NG  
22  
23 combustion, we also explore, briefly, the potential success of several, comprehensive  
24  
25 kinetic models that have been developed for methane combustion in reproducing the  
26  
27 ignition delays that we have measured using natural gas.  
28  
29  
30  
31  
32

### 33 34 *Previous related studies*

35  
36 Ignition delay measurements and numerical simulations have been made of the  
37  
38 effect of hydrogen addition on the combustion of methane in shock tubes [18-21] and  
39  
40 a rapid compression machine [22]. The investigation by Zhang et al [21] covers a  
41  
42 complete composition range (100% CH<sub>4</sub> to 100% H<sub>2</sub> as fuel) at pressures from 5 – 20  
43  
44 bar and temperatures from 1020 – 1750 K, and is accompanied by extensive  
45  
46 numerical simulations and kinetic analyses. In each of these studies [18-22], an  
47  
48 increase of the global rate of oxidation at any given temperature was observed when  
49  
50 hydrogen was added in increasing proportions.  
51  
52

53  
54 Recently, with interests in the use of syngas, Gersen *et al* [23] measured ignition  
55  
56 delays of stoichiometric and fuel-lean mixtures, comprising H<sub>2</sub>, H<sub>2</sub>/CO, CH<sub>4</sub>, CH<sub>4</sub>/CO,  
57  
58  
59  
60

1  
2  
3 CH<sub>4</sub>/H<sub>2</sub> and CH<sub>4</sub>/CO/H<sub>2</sub>, in an RCM at pressures ranging from 20 to 80 bar over the  
4  
5 compressed gas temperature range 900–1100 K. Ignition delays were shortest for H<sub>2</sub>  
6  
7 under comparable conditions to other mixtures, and those of CH<sub>4</sub> were the longest.  
8  
9 The replacement of 30% CH<sub>4</sub> by H<sub>2</sub> had a significant effect on CH<sub>4</sub> ignition, the  
10  
11 delays falling between those of the single component fuels. The effects of CO, at  
12  
13 50% of the fuel with H<sub>2</sub> and at 20% of the fuel with both CH<sub>4</sub> and CH<sub>4</sub>/H<sub>2</sub> mixtures,  
14  
15 were found to be negligible. The addition of syngas to CH<sub>4</sub> resulted in ignition  
16  
17 behavior that resembled an equivalent CH<sub>4</sub>/H<sub>2</sub> mixture containing the same H<sub>2</sub>  
18  
19 fraction. The experimental observations were reproduced satisfactorily in numerical  
20  
21 simulations.  
22  
23

24  
25 Although a helpful approach because it simplifies the interpretation of the kinetic  
26  
27 effects, the study of methane as a surrogate for NG has limitations because, in  
28  
29 reality, the heavier hydrocarbons that are present in NG also have a marked  
30  
31 influence on methane oxidation. Thus, a complementary investigation of the ignition  
32  
33 response of NG to the inclusion of EGR and syngas components is appropriate.  
34  
35

36  
37 However, little kinetic work has been done so far using natural gas/hydrogen  
38  
39 mixtures. Dagaut and Dayma [24] studied the kinetics of oxidation of CH<sub>4</sub>/C<sub>2</sub>H<sub>6</sub>/H<sub>2</sub>  
40  
41 mixtures in a high pressure (10 atm) Jet-Stirred Reactor (JSR), between 900 and  
42  
43 1200 K. They showed that the oxidation of the CH<sub>4</sub>/C<sub>2</sub>H<sub>6</sub> mixture is enhanced by the  
44  
45 addition of H<sub>2</sub>, and attribute the reactivity enhancement to an increase in the  
46  
47 concentrations of H<sup>•</sup>, ·OH and HO<sub>2</sub><sup>•</sup> radicals when hydrogen is present in the initial  
48  
49 mixtures. De Ferrières et al. [25] added 20 to 60% H<sub>2</sub> to NG in a low pressure flat  
50  
51 flame and measured the concentration profiles of the reactants and products in order  
52  
53 to study the kinetic effects of hydrogen addition. Their conclusion was that, under  
54  
55  
56  
57  
58  
59  
60

1  
2  
3 their conditions, the channels involving H-abstraction by H $\cdot$  atoms are increasingly  
4 favoured, as is the formation of CO over CO $_2$ .  
5

6  
7 Prior to the work reported in [23] the ignition of pure H $_2$ /O $_2$  and H $_2$ /CO/O $_2$  mixtures  
8 was investigated in an RCM by Mittal et al. [26] under a wide range of experimental  
9 conditions, and the kinetic importance of HO $_2\cdot$  radicals and of H $_2$ O $_2$  was emphasised  
10 through numerical simulation.  
11

12  
13 The large heat capacity of carbon dioxide, compared to that of nitrogen or argon, has  
14 led to its frequent use as an inert gas for RCM studies under 700 K [27]. But the  
15 effect of CO $_2$  blending on CH $_4$  ignition at higher temperatures is limited to the study of  
16 the addition of large quantities of CO $_2$  to CH $_4$ /air mixtures in a JSR at 10 atm,  
17 between 900 and 1450 K, by Le Cong and Dagaut [28]. They showed that CO $_2$  has a  
18 thermal effect which reduces flame temperatures, as well as a chemical effect that is  
19 likely to proceed through the reduction of the concentration of H $\cdot$  atoms via CO $_2$  + H $\cdot$   
20 = CO +  $\cdot$ OH.  
21  
22

23  
24 To our knowledge, there are no reported studies on the effect of added water on the  
25 ignition delay of NG, although Christensen and Johansson [29] have shown that the  
26 addition of water could be used to delay the ignition time in an HCCI engine fuelled  
27 with natural gas.  
28  
29

## 30 31 32 33 34 35 36 37 38 39 40 41 42 43 44 45 **2. Experimental**

46  
47  
48  
49 The experiments were carried out in the RCM at the University of Lille. This RCM has  
50 a right-angle design, which ensures that the volume is kept strictly constant at the  
51 end of the compression. The full details of this facility have been described elsewhere  
52 [9,27,30-32]. The pressure profiles during operation of the RCM are measured by a  
53  
54  
55  
56  
57  
58  
59  
60

1  
2  
3 Kistler 601A piezoelectric pressure transducer with a 40  $\mu$ s time step. The ignition  
4 delay time is defined as the time between the end of the compression (TDC: Top  
5 Dead Centre) and the maximum rise of the pressure associated with ignition. The  
6  
7 core gas temperature ( $T_C$ ) is calculated following the adiabatic core model from the  
8  
9 pressure at TDC and the initial conditions [30,33,34]. The compression ratio was 11:1  
10  
11 and the cylinder and combustion temperature walls were maintained at 90 °C.  
12  
13

14  
15 The gas mixtures were prepared in a glass mixing facility, using the partial pressures  
16  
17 method, and left to homogenise overnight. The dilution of all mixtures by inert gases  
18  
19 ( $N_2$ , Ar) was identical to that of the proportion of  $N_2$  in air. The natural gas used in this  
20  
21 study was composed of 89% methane, 9% ethane and 2% propane. The gases were  
22  
23 provided by Air Liquide with the following purities: NG (9.00  $\pm$  0.18%  $C_2H_6$ , 2.00  $\pm$   
24  
25 0.18%  $C_3H_8$  in  $CH_4$ ),  $CH_4$  (99.95%),  $H_2$  (99.999%),  $O_2$ ,  $N_2$  and Ar (99.99%), CO  
26  
27 (99.91%),  $CO_2$  (99.95%). Carbon monoxide was stored in an aluminium cylinder to  
28  
29 avoid  $Fe(CO)_5$  formation [35]. The composition of the  $N_2/Ar$  inert gas mixture was  
30  
31 varied, so changing the ratio of heat capacities in order to reach the different core  
32  
33 gas temperatures investigated.  
34  
35

36  
37 Mixtures containing  $H_2O$  were prepared in a heated mixture preparation facility [36] to  
38  
39 avoid its condensation. Its temperature was fixed at 80 °C, and the tubing between  
40  
41 the facility and the RCM was also heated to 80 °C. At this temperature, the vapour  
42  
43 pressure of water is more than 47 kPa, whereas the maximum water partial pressure  
44  
45 used during mixture preparation was less than 5 kPa. The water was purified from  
46  
47 dissolved gases by several freezing/pumping cycles.  
48  
49

50  
51 It has been shown earlier [35] that when measuring ignition delays in the presence of  
52  
53  $H_2$ , non-uniform ignition can be a major concern, and the presence of particles has  
54  
55 been discussed as a possible cause for these non-uniform ignitions. To avoid this  
56  
57  
58  
59  
60

1  
2  
3  
4  
5  
6  
7  
8  
9  
10  
11  
12  
13  
14  
15  
16  
17  
18  
19  
20  
21  
22  
23  
24  
25  
26  
27  
28  
29  
30  
31  
32  
33  
34  
35  
36  
37  
38  
39  
40  
41  
42  
43  
44  
45  
46  
47  
48  
49  
50  
51  
52  
53  
54  
55  
56  
57  
58  
59  
60

eventuality a Millipore filter (0.5  $\mu\text{m}$ ) was installed between the gas mixture preparation facility and the RCM. No difference was observed between results performed with and without the filter for the mixture with the highest hydrogen content. As a consequence, most of the experiments were performed without utilizing the filter.

Non-reactive pressure profiles were acquired for each reactive mixture by replacing  $\text{O}_2$  by  $\text{N}_2$ . These profiles reveal the rate and extent of the pressure fall due to cooling in the boundary layer after the end of compression and they enable an accurate reproduction of the heat loss, based on adiabatic expansion of the core gas, to be obtained in zero-dimensional simulations [37]. The corresponding mixture compositions and “thermal diffusivity” values, as well as the non-reactive pressure profiles, are available from the authors for all mixtures studied.

The right-angle design of this RCM allows the compression time to be varied without changing the compression ratio. The influence of the compression time on natural gas ignition was therefore investigated, as shown in Section 3. Following the recommendations of Lee and Hochgreb [38], a creviced piston head was used, to ensure maximum homogeneity of the temperature field in the core gas at the end of the compression.

### 3. Experimental Results

A comparison of a reactive and a non-reactive pressure profile is presented for an NG/ $\text{H}_2$  mixture, in Figure 1. Heat release during the development of autoignition is sufficiently small for there to be no discernible difference in the pressure profiles until a relatively late stage. Figure 2 sums up the results obtained for the effect of the

1  
2  
3 variation of the compression time on ignition delay measurement. At high piston  
4  
5 velocities, it shows variations of the TDC pressure increase, and also that the  
6  
7 decrease of the pressure after TDC occurs in two distinct phases. This is partly due  
8  
9 to vibration which induces a periodic perturbation of the pressure signal, but also  
10  
11 from possible non-ideal effects such as turbulence dissipation, and consequent  
12  
13 mixing of the adiabatic core with the boundary layer. Adequate reproduction of the  
14  
15 heat loss with the core gas expansion model [37] is then made very difficult. At the  
16  
17 other extreme, too long a compression time would increase the opportunity for  
18  
19 reaction to occur during the compression phase. A compression time of 60 ms was  
20  
21 therefore chosen, as in previous work [9,27,30-32].  
22  
23

24  
25 A comparison of ignition data obtained with a flat piston and a creviced piston was  
26  
27 performed at a compression time of 60 ms, as shown on Figure 3. The ignition delays  
28  
29 using the flat piston appear to be slightly longer than those with the creviced piston,  
30  
31 suggesting that there is a limited effect of a roll up vortex. These experimental results  
32  
33 were simulated using the NUIG mechanism [16]. The simulation results are also  
34  
35 plotted in Figure 3, and show little difference between the flat piston and the creviced  
36  
37 piston results. The modelling of the results using core gas expansion into the  
38  
39 boundary layer gives acceptable results in both cases [37].  
40  
41

42  
43 Measurements of ignition delay for a range of reactive mixtures, using the creviced  
44  
45 piston crown, are shown in Figures 4-11 and presented in the following sub-sections,  
46  
47 The lines are included as  $\beta$ -spline fits to the experimental data, and the indicated  
48  
49 pressures are the minimum and maximum values reached at TDC. The compressed  
50  
51 gas pressure variation results from the increased gas temperature for a fixed initial  
52  
53 pressure of each composition, in the range 80.0 - 106.7 kPa, as the heat capacity of  
54  
55 the mixture is decreased.  
56  
57  
58  
59  
60

### *Methane*

Autoignition delay times for stoichiometric ( $\Phi = 1.0$ ) methane/"air" mixtures and at  $\Phi = 0.7$  have been measured. Their variation with  $T_C$  was investigated over the temperature range 880 - 1000 K at compressed gas pressures in the range 20.5 - 22.7 bar, as presented in Figure 4. The studies of stoichiometric CH<sub>4</sub>/"air" mixtures were restricted to an upper compressed gas temperature of 950 K at the given compression ratio, as a result of their higher overall heat capacity relative to those for the compositions at  $\Phi = 0.7$  (Figure 4), for which 1000 K could be reached. Ignition delays are longer for  $\Phi = 0.7$  mixtures, especially at the lower temperatures. This is consistent with the results of Healy et al. [7].

In this and other cases, at the lowest compressed gas temperature for ignition the ignition delay becomes very sensitive to variation between experiments, as its duration tends asymptotically to infinity. This scatter of the data may also be influenced by a gradual reduction of the core volume owing to heat loss competing with the low exothermicity of reaction, in the early stages of the ignition delay.

### *Natural Gas*

Figure 5 shows the decrease of the ignition delays of stoichiometric NG/"air" mixtures with increasing  $T_C$  at three different initial pressures. Ignition was still possible at  $T_C < 900$  K, at the higher initial pressures, but it was not observed below 915 K at an initial pressure of 80 kPa. The enhanced reactivity of NG in a stoichiometric mixture relative to that at  $\phi = 0.7$  is presented in Figure 6.

1  
2  
3 A comparison between the measured ignition delays for stoichiometric CH<sub>4</sub>/"air" and  
4 NG/"air" mixtures, in Figure 7, demonstrates the marked sensitisation of methane  
5 autoignition to the presence of ethane (9%) and propane (2%).  
6  
7  
8  
9

#### 10 11 *Natural gas blending with hydrogen*

12  
13 The effect of hydrogen blending to natural gas has been studied for fuel fractions  
14  $x_{H_2}/(x_{H_2}+x_{NG}) = 0.2$  and  $0.6$ . The measured ignition delays are plotted as a function of  
15  $T_C$  in Figure 8: That the presence of hydrogen reduces the ignition delay of natural  
16 gas is clear, but there are interesting, additional features. That is, there is a  
17 significant reduction of the ignition delay when NG is replaced by 20% H<sub>2</sub> but the  
18 sensitivity to a further increase of H<sub>2</sub> to 60% is very slight. Moreover, from the data  
19 obtained either side of  $T_C \sim 905$  K at the two compositions, the reproducibility of the  
20 experiments is sufficiently good to show a cross-over of the ignition delay  
21 dependence on the proportion of H<sub>2</sub>. The 80/20 NG/H<sub>2</sub> mixture appears to be the less  
22 reactive mixture below 905 K, as expected, but the slightly more reactive of the two  
23 above this temperature.  
24  
25  
26  
27  
28  
29  
30  
31  
32  
33  
34  
35  
36  
37  
38  
39

#### 40 *Natural gas blending with carbon monoxide*

41  
42 In order to evaluate the effect of carbon monoxide on the ignition delays of natural  
43 gas, a partial substitution of NG by CO was made, at fuel proportions ranging from 10  
44 to 30% in the reactant mixture, while keeping the equivalence ratio constant at  $\phi =$   
45 1.0. The ignition delays are plotted as a function of  $T_C$  on Figure 9. Carbon monoxide  
46 appears to have no discernible effect on the ignition delays of natural gas.  
47  
48  
49  
50  
51  
52  
53  
54  
55  
56  
57  
58  
59  
60

### *Natural gas blending with carbon dioxide*

Several NG/CO<sub>2</sub> mixtures were studied by addition of CO<sub>2</sub> up to  $x_{CO_2}/(x_{NG}+x_{CO_2}) = 0.3$ , the equivalence ratio of the NG being kept constant. At its highest proportion, the CO<sub>2</sub> constitutes about 4% by volume of the total reactant mixture. This has a small effect of increasing the overall heat capacity and so decreases the temperature reached at the end of compression to a limited extent. As can be seen on Figure 10, no effect on the ignition delay could be discerned. The proportion is very low compared with the 20% mole fraction of CO<sub>2</sub> in the mixtures studied by Le Cong and Dagaut [28]. Adding a compound with a relatively high heat capacity to the mixture is likely to have an effect on the variation of temperature induced by the heat release. This can result in a variation of the ignition delays, as described by Würmel et al. [39], but no such effect was observed in our conditions with relatively low CO<sub>2</sub> mole fractions.

### *Natural gas blending with Water*

Water was introduced in our mixtures, in a way similar to that of CO<sub>2</sub>, at a proportion of 30% relative to the fuel. As shown on Figure 11, there appears to be no effect of water addition on the ignition delay at compressed gas temperatures above 910 K. However, as in the case of CO<sub>2</sub>, there is a reduction of the core gas temperatures reached at the end of the compression as a result of the addition of water to the mixtures.

### *Summary of the effects of EGR components*

The results obtained with all of the EGR components are summarised in Figure 12, for T<sub>C</sub> between 917 and 936 K. The core gas temperatures were not strictly identical

1  
2  
3 for different additive fuel fractions because the heat capacities of each fuel/additive  
4  
5 mixture varied to a limited extent. This small variation in  $T_C$  was sufficient to affect the  
6  
7 measured ignition delays through the overall activation energy of the reaction rate,  
8  
9 and this accounts for the scatter in the case of  $H_2O$  and  $CO_2$  blending, which is  
10  
11 marked within the grey zone in Figure 12. This marked zone corresponds to an  
12  
13 increase or a decrease of the ignition delay by less than 20%. Only hydrogen has a  
14  
15 discernible effect in reducing the ignition delay, as the proportion of hydrogen in the  
16  
17 fuel was increased from 0 to 60%. The other additives hardly influence the ignition  
18  
19 delay, up to proportions equivalent to 30% of the fuel.  
20  
21  
22  
23  
24

#### 25 **4. Discussion**

26  
27  
28

29  
30 By virtue of the presence of higher alkanes (9 mol%  $C_2H_6$  and 2 mol%  $C_3H_8$ ) the  
31  
32 significant enhancement of the autoignition of NG relative to that of  $CH_4$  is evident  
33  
34 throughout the temperature range investigated in the present experiments. There is  
35  
36 further enhancement of the reactivity when  $H_2$  is substituted for NG, albeit with a  
37  
38 much reduced sensitivity at high proportions of  $H_2$ . The lack of sensitivity to the  
39  
40 replacement of NG by CO shows that CO plays some part in the kinetics and heat  
41  
42 release in the overall reaction. If CO were to act predominantly as an inert diluent,  
43  
44 then we would expect there to be an increase in the ignition delay consistent with the  
45  
46 response of NG at  $\phi = 0.7$  relative to that of NG at  $\phi = 1.0$ . This is corroborated by  
47  
48 Mittal et al [40], who showed that the ignition delay in  $H_2/N_2$  mixtures was longer than  
49  
50 that in corresponding  $H_2/CO$  compositions, at above 1000 K, especially when the  
51  
52 proportion of CO or  $N_2$  exceeded 50% of the 'fuel' component. The behaviour of NG  
53  
54 in the presence of CO observed in the present work is similar to ignition data  
55  
56  
57  
58  
59  
60

1  
2  
3 obtained by Gersen *et al* [23], both for CH<sub>4</sub>/CO and H<sub>2</sub>/CO mixtures relative to those  
4  
5 from CH<sub>4</sub> and H<sub>2</sub> respectively. By contrast, at the extreme, the sensitization of CO  
6  
7 ignition by very small amounts of H<sub>2</sub>, or other hydrogenous compounds, has been  
8  
9 known for a considerable time and is well documented [41].  
10

#### 11 12 13 14 *Tests of methane kinetic models applied to natural gas autoignition*

15  
16 The purpose of this final part of our discussion is to explore the extent to which  
17  
18 various comprehensive kinetic models for methane combustion may be applied  
19  
20 successfully to the simulation of the present experimental measurements of ignition  
21  
22 delay involving a natural gas of known composition.  
23

24  
25 The simulations were performed using the Chemkin package [42], assuming time-  
26  
27 dependent volume profile to simulate the expansion of the core gas into the boundary  
28  
29 layer [37]. The natural gas composition used in the simulations comprised  
30  
31 methane/ethane/propane = 89/9/2%, as in the experiments. Four models were  
32  
33 considered: The LENI model [9], the NUIG model [16], the USC model [43], and the  
34  
35 GRI 3.0 model with the RAMEC sub-mechanism [44,45].  
36

37  
38 In previous work, the LENI model has been tested against RCM data using a  
39  
40 synthetic methane/ethane/propane mixture with a similar composition to the present  
41  
42 NG [9]. The NUIG model has been validated on a large number of mixtures, including  
43  
44 90/6.6/3.3, 70/15/15, and 70/20/10 methane/ethane/propane mixtures, expressed as  
45  
46 percentages, as well as mixtures containing higher hydrocarbons [7]. The USC model  
47  
48 has been applied to a large variety of high-temperature ignition delay measurements  
49  
50 for hydrogen and single component C<sub>1</sub> to C<sub>3</sub> hydrocarbons [21]. The RAMEC sub-  
51  
52 mechanism has been developed to extend the validation of the GRI mechanism to  
53  
54 intermediate temperatures shock tube methane ignition delays [45].  
55  
56  
57  
58  
59  
60

1  
2  
3 The comparison between the experimental and the simulated ignition delays is  
4 presented in Figure 13. It shows that the present natural gas results are best  
5 simulated by the NUIG model, with which the agreement, for a stoichiometric mixture,  
6 is very good throughout the pressures and temperature ranges investigated. The  
7 simulation of experimental investigations of CH<sub>4</sub> autoignition, to which similar  
8 components were blended, also gives a very satisfactory validation of the NUIG  
9 model [23]. There is a reasonable representation of the present NG data using the  
10 LENI model, albeit with a consistent under-prediction of the ignition delay by  
11 approximately 50%. It is conspicuous that the models that have not been set up with  
12 adequate representation of the kinetic interactions involving ethane and propane do  
13 not, generally, predict sufficiently high reactivity and fail to capture the combustion  
14 leading to ignition at the lowest core gas temperatures.

15  
16  
17  
18  
19  
20  
21  
22  
23  
24  
25  
26  
27  
28  
29  
30 In a supplementary analysis, simulations were made to explore the extent to which  
31 reaction may occur during the compression phase, based on the velocity profile of  
32 the piston, and comparing the results with the non-compression simulation adopted in  
33 the earlier calculations. The position - time profile of the experiments is available from  
34 the authors on request. As shown in Figure 14, whereas there is no evidence of  
35 significant reaction having started during the compression phase of NG alone, the  
36 decrease of the predicted ignition delay in the case of NG-H<sub>2</sub> mixtures indicates that  
37 some reactivity has occurred during the compression phase.

38  
39  
40  
41  
42  
43  
44  
45  
46  
47 Finally, the precision with which the effect of EGR components can be predicted  
48 using the NUIG model [16] was explored briefly by reference to the data presented in  
49 Figure 12. The simulations took into account the possibility of reaction in the  
50 compression stroke in the case of hydrogen-containing mixtures. As shown in Figure  
51 15, the predicted ignition delays of increasing proportions of CO<sub>2</sub>, CO and H<sub>2</sub>O in  
52  
53  
54  
55  
56  
57  
58  
59  
60

1  
2  
3 NG/CO<sub>2</sub>, NG/CO and NG/H<sub>2</sub>O mixtures show very little effect on the reactivity of NG.  
4  
5 The enhanced reactivity in the presence of increasing proportions of H<sub>2</sub> is clearly  
6  
7 demonstrated, although the duration of the ignition delay is over-estimated by the  
8  
9 model. This may suggest that further model development may be required on the  
10  
11 interactions between the kinetic mechanisms between the two fuel components.  
12  
13

## 14 15 16 **5. Conclusions** 17

18  
19  
20 A detailed experimental study of the autoignition of methane, natural gas and natural  
21  
22 gas with various additional components, typical of those associated with exhaust gas  
23  
24 recirculation, was performed in an RCM. Ignition delays of pure methane/"air"  
25  
26 mixtures were measured and found to increase from equivalence ratios 1.0 to 0.7.  
27  
28 These results were compared with those from natural gas, which ignites with a  
29  
30 shorter ignition delay at all conditions investigated. Blending hydrogen in the mixture  
31  
32 at all volume percentages in the fuel from 20 to 60% shortens the ignition delay. CO  
33  
34 was found to have no effect up to a fuel proportion of 30%. Simulations were  
35  
36 performed with the NUIG mechanism: the agreement is overall very good for natural  
37  
38 gas and the different additives. In order to be able to reproduce the effect of EGR in  
39  
40 real engines conditions, further work might be required to improve the simulation of  
41  
42 H<sub>2</sub>-containing mixtures.  
43  
44  
45  
46  
47  
48

## 49 50 **6. Acknowledgements** 51

52 The authors would like to thank GDF SUEZ CRIGEN and the Institut de Recherche  
53  
54 en ENvironnement Industriel (IRENI) for financial support of this project. IRENI is  
55  
56  
57  
58  
59  
60

1  
2  
3  
4  
5  
6  
7  
8  
9  
10  
11  
12  
13  
14  
15  
16  
17  
18  
19  
20  
21  
22  
23  
24  
25  
26  
27  
28  
29  
30  
31  
32  
33  
34  
35  
36  
37  
38  
39  
40  
41  
42  
43  
44  
45  
46  
47  
48  
49  
50  
51  
52  
53  
54  
55  
56  
57  
58  
59  
60

funded by the Région Nord Pas-de-Calais, the Ministère de l'Enseignement Supérieur et de la Recherche, the CNRS and FEDER.

**References**

- [1] T. Korakianitis, A.M. Namasivayam, R.J. Crookes, *Prog. Energ. Combust.* 37 (2011) 89-112.
- [2] M.C. Seemann, T.J. Schildhauer, S.M.A. Biollaz, *Ind. Eng. Chem. Res.* 49 (2010) 7034–7038.
- [3] J. Kopyscinski, T.J. Schildhauer, S.M.A. Biollaz, *Fuel* 89 (2010) 1763-1783.
- [4] R.W.R. Zwart, A. Drift, 15th European Biomass Conference and Exhibition, Berlin, Germany, 2007, p.7-11.
- [5] A. El Bakali, P. Dagaut, L. Pillier, P. Desgroux, J.-F. Pauwels, A. Rida, P. Meunier, *Combust. Flame* 137 (2004) 109-128.
- [6] E.L. Petersen, D.M. Kalitan, S. Simmons, G. Bourque, H.J. Curran, J.M. Simmie, *Proc. Combust. Inst.* 31 (2007) 447-454.
- [7] D. Healy, H.J. Curran, J.M. Simmie, D.M. Kalitan, C.M. Zinner, A.B. Barrett, E.L. Petersen, G. Bourque, *Combust. Flame* 155 (2008) 441-448.
- [8] D. Healy, H.J. Curran, S. Dooley, J.M. Simmie, D.M. Kalitan, E.L. Petersen, G. Bourque, *Combust. Flame* 155 (2008) 451-461
- [9] S. Heyne, A. Roubaud, M. Ribaucour, G. Vanhove, R. Minetti, D. Favrat, *Fuel* 87 (2008) 3046-3054.
- [10] C.S. Eubank, M.J. Rabinowitz, W.C. Gardiner Jr, R.E. Zellner, *Proc. Combust. Inst.* 18 (1981) 1767-1774.
- [11] N. Lamoureux, C.E. Paillard, *Shock Waves* 13 (2003) 57-68.
- [12] L.J. Spadaccini and M.B. Colkett, *Prog. Energy. Combust. Sci.* 20 (1994) 431-460
- [13] R.M.R. Higgins, A. Williams, *Proc. Combust. Inst.* 12 (1969) 579-590.

- 1  
2  
3 [14] R.W. Crossley, E.A. Dorko, K. Scheller, A. Burcat, *Combust. Flame* 19 (1972)  
4  
5 373-378.  
6  
7 [15] M. Frenklach, D.E. Bornside, *Combust. Flame* 56 (1984) 1-27.  
8  
9 [16] D. Healy, D.M. Kalitan, C.J. Aul, E.L. Petersen, G. Bourque, H. J. Curran, *Energy*  
10  
11 *Fuels* 24 (2010) 1521-1528.  
12  
13 [17] G.A. Karim, I. Wierzba, Y. Al-Alousi, *Int. J. Hydrogen Energy* 21 (1996) 625-631.  
14  
15 [18] N. Chaumeix, S. Pichon, F. Lafosse, C-E. Paillard, *Int. J. Hydrogen Energy* 32  
16  
17 (2007) 2216-2226.  
18  
19 [19] J. Huang, W.K. Bushe, P.G. Hill, S.R. Munshi, *Int. J. Chem. Kinet.* 38 (2006)  
20  
21 221–233.  
22  
23 [20] E.L. Petersen, J.M. Hall, S.D. Smith, J. de Vries, A.R. Amadio, M.W. Crofton, J.  
24  
25 *Eng. Gas. Turb. Power* 129 (2007) 937-944.  
26  
27 [21] Y. Zhang, Z. Huang, L. Wei, J. Zhang, C. K. Law, *Combust. Flame* 159 (2012)  
28  
29 918-931.  
30  
31 [22] S. Gersen, N.B. Anikin, A.V. Mokhov, H.B. Levinsky, *Int. J. Hydrogen Energy* 33  
32  
33 (2008) 1957-1964.  
34  
35 [23] S. Gersen, H. Darneveil, H. Levinsky, *Combust. Flame* 159 (2012) 3472 - 3475.,  
36  
37 [24] P. Dagaut, G. Dayma, *Int. J. Hydrogen Energy* 31 (2006) 505-515.  
38  
39 [25] S. de Ferrières, A. El Bakali, B. Lefort, M. Montero, J.-F. Pauwels, *Combust.*  
40  
41 *Flame* 154 (2008) 601-623.  
42  
43 [26] G. Mittal, C-J. Sung, R. A. Yetter, *Int. J. Chem. Kinet.* 38 (2006) 516–529.  
44  
45 [27] R. Minetti, M. Carlier, M. Ribaucour, E. Therssen, L.R. Sochet, *Proc. Combust.*  
46  
47 *Inst.* 26 (1996) 747-753.  
48  
49 [28] T. Le Cong, P. Dagaut, *Combust. Sci. Technol.* 180 (2008) 2046-2091.  
50  
51 [29] M. Christensen, B. Johansson, SAE paper SAE1999-01-0182, 1999.  
52  
53  
54  
55  
56  
57  
58  
59  
60

- 1  
2  
3 [30] R. Minetti, M. Ribaucour, M. Carlier, C. Fittschen, L.R. Sochet, *Combust. Flame*  
4 96 (1994) 201-211.  
5  
6  
7 [31] R. Minetti, M. Carlier, M. Ribaucour, E. Therssen, L.R. Sochet, *Combust. Flame*  
8 102 (1995) 298-309.  
9  
10  
11 [32] R. Minetti, M. Ribaucour, M. Carlier, L.R. Sochet, *Combust. Sci. Technol.* 113-  
12 114 (1996) 179-192.  
13  
14  
15 [33] P. Desgroux, L. Gasnot, L.R. Sochet, *Appl. Phys.* 61 (1995) 69-72.  
16  
17  
18 [34] C.K. Westbrook, H.J. Curran, W.J. Griffiths, C. Mohamed, S.K. Wo, *Proc.*  
19 *Combust. Inst.* 27 (1998) 371-378.  
20  
21  
22 [35] M. Chaos, F.L. Dryer, *Combust. Sci. Technol.* 180 (2008) 1053-1096.  
23  
24 [36] M. Crochet, R. Minetti, M. Ribaucour, G. Vanhove, *Combust. Flame* 157 (2010)  
25 2078-2085.  
26  
27  
28 [37] S. Tanaka, F. Ayala, J.C. Keck, *Combust. Flame* 133 (2003) 467-481.  
29  
30  
31 [38] D. Lee, S. Hochgreb, *Combust. Flame*, 114 (1998) 531-545.  
32  
33  
34 [39] J. Würmel, E.J. Silke, H.J. Curran, M.S. Ó Conaire, J.M. Simmie, *Combust.*  
35 *Flame* 151 (2007) 289-302.  
36  
37  
38 [40] G.Mittal, C.J. Sung, M. Fairweather, A.S. Tomlin, J.F. Griffiths, K.J. Hughes,  
39 *Proc. Comb. Inst.* 31, 419-427 (2007)  
40  
41  
42 [41] B. Lewis, G. Von Elbe, "Combustion, Flames and Explosions in Gases, 3<sup>rd</sup>  
43 Edition", Academic Press, Orlando, 1987, ISBN 0-12-446751-2  
44  
45  
46 [42] R.J. Kee, F.M. Rupley, J.A. Miller, CHEMKIN-II: A Fortran Chemical Kinetics  
47 Package for the Analysis of Gas-Phase Chemical Kinetics, Report NO. SAND 89-  
48 8009B, Sandia National Laboratories, 1991.  
49  
50  
51 [43] H. Wang, X. You, A.V. Joshi, S.G. Davis, A. Laskin, F. Egolfopoulos, C.K. Law,  
52 available at <[http://ignis.usc.edu/USC\\_Mech\\_II.htm](http://ignis.usc.edu/USC_Mech_II.htm)>.  
53  
54  
55  
56  
57  
58  
59  
60

1  
2  
3 [44] M. Frenklach, H. Wang, C-L. Yu, M. Goldenberg, C.T. Bowman, R.K. Hanson,  
4  
5 D.F. Davidson, E.J. Chang, G.P. Smith, D.M. Golden, W.C. Gardiner, V. Lissianski,  
6  
7 available at <[http://www.me.berkeley.edu/gri\\_mech/](http://www.me.berkeley.edu/gri_mech/)>.  
8

9  
10 [45] E.L. Petersen, D.F. Davidson, R.K. Hanson, Combust. Flame 117 (1999) 272–  
11  
12 290.  
13  
14  
15  
16  
17  
18  
19  
20  
21  
22  
23  
24  
25  
26  
27  
28  
29  
30  
31  
32  
33  
34  
35  
36  
37  
38  
39  
40  
41  
42  
43  
44  
45  
46  
47  
48  
49  
50  
51  
52  
53  
54  
55  
56  
57  
58  
59  
60

## Figures

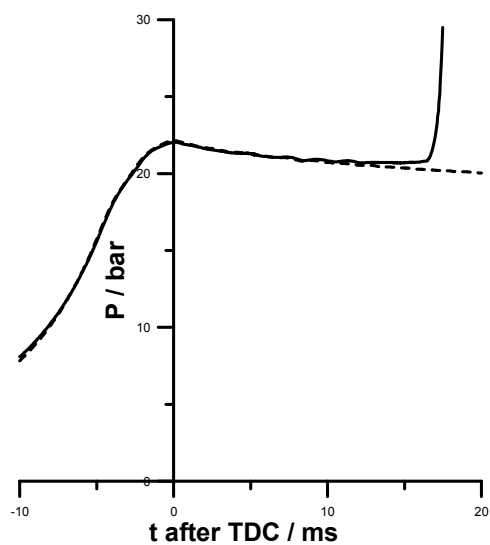


Figure 1

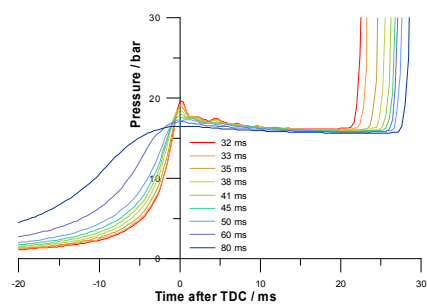


Figure 2. To be printed in colour

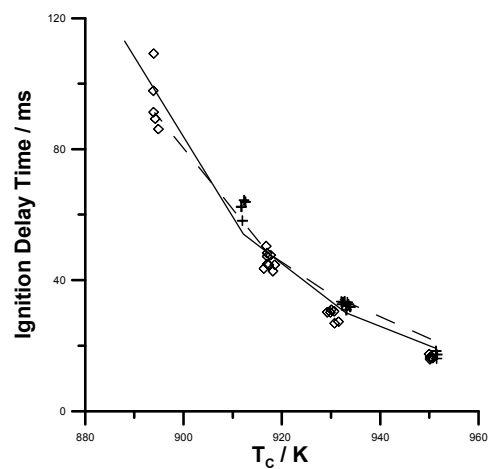


Figure 3

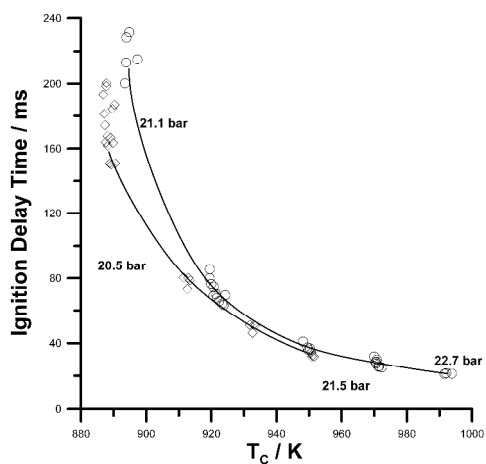


Figure 4

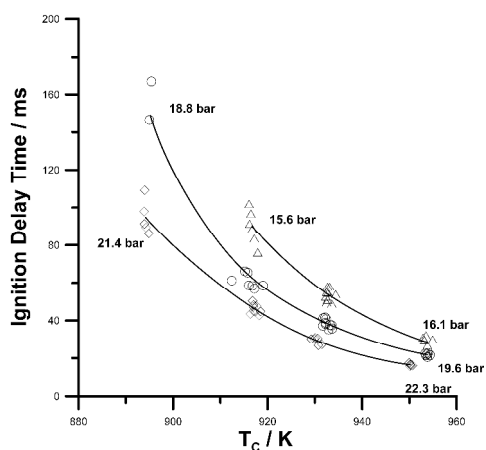


Figure 5

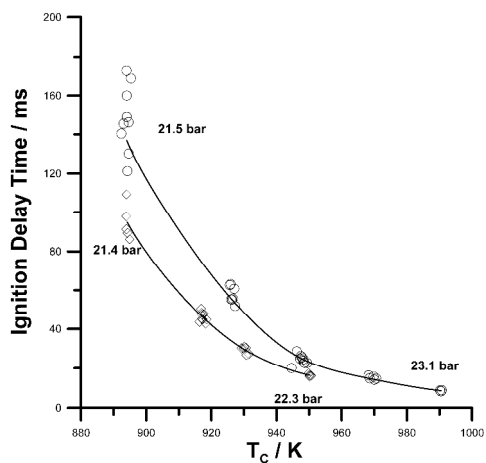


Figure 6

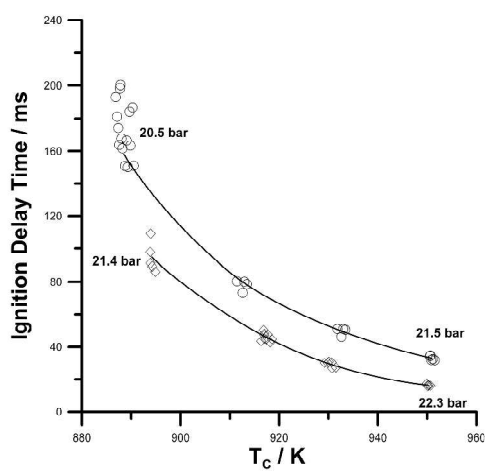


Figure 7

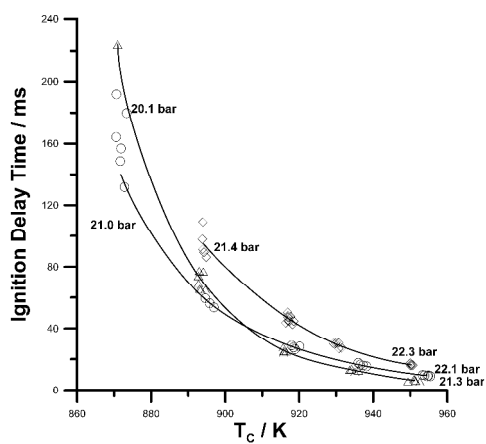


Figure 8

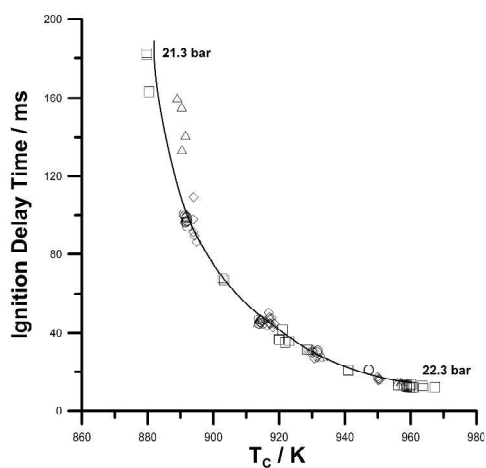


Figure 9

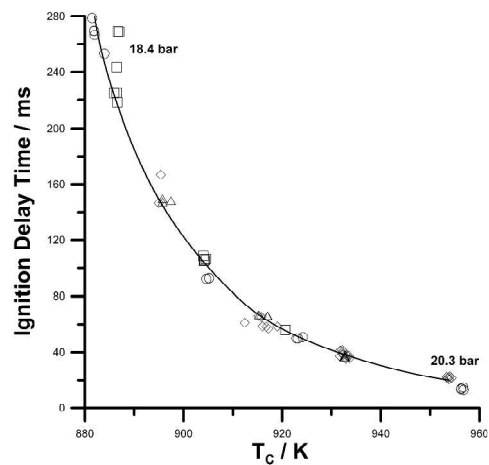


Figure 10

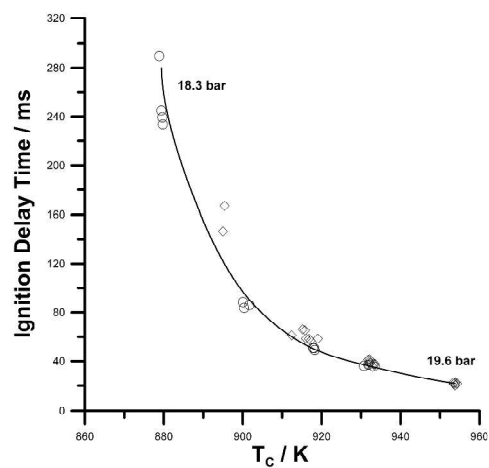


Figure 11

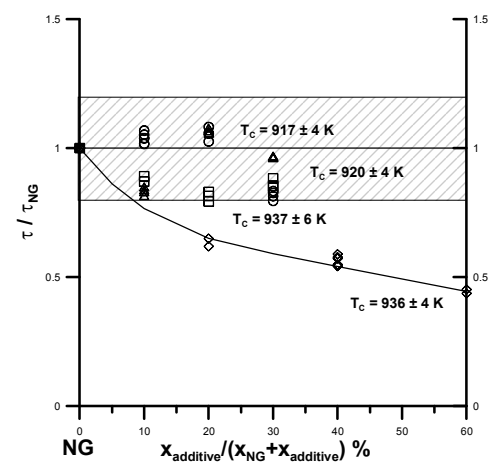


Figure 12

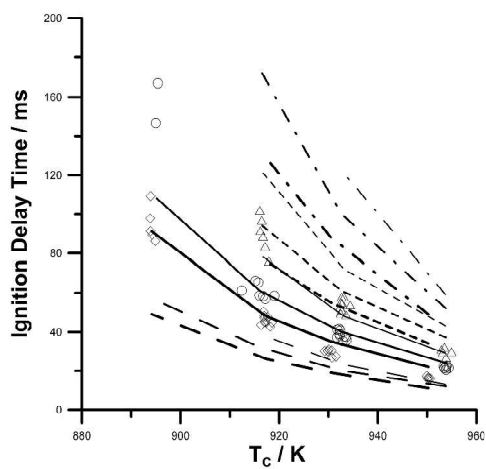


Figure 13

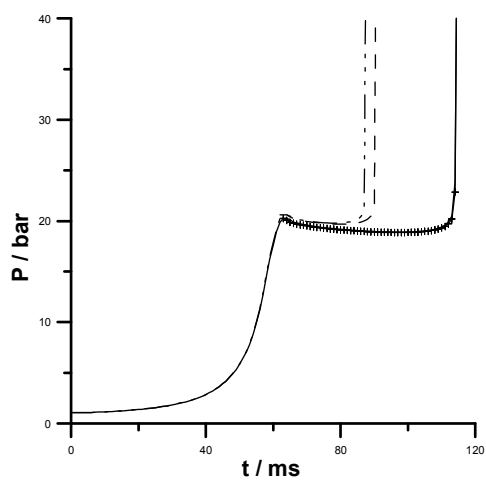


Figure 14

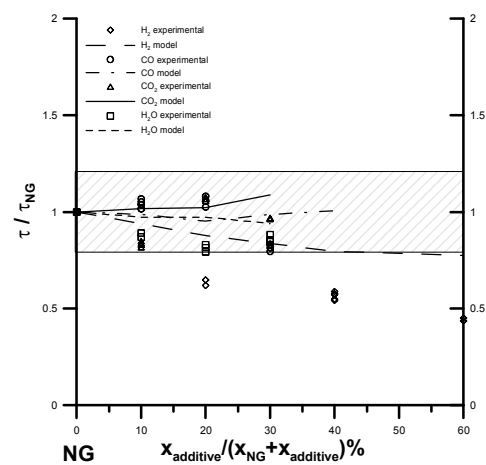


Figure 15

## Figures Captions

Figure 1: Comparison of the reactive (full line) and the non-reactive (dashed line) pressure profiles in the case of the compression of a NG/H<sub>2</sub>(80/20)/"air" mixture.

Initial pressure  $P_0 = 106.7$  kPa, compression time 60 ms.

Figure 2: Effect of the compression time on the pressure profile during a reactive NG/O<sub>2</sub>/Ar experiment.  $P_0 = 80$  kPa.

Figure 3: Comparison of the measured (points) and simulated (lines) evolution of the ignition delay times of stoichiometric synthetic natural gas/O<sub>2</sub>/inert mixtures as a function of  $T_C$ , for two piston configurations: crosses, full line: flat piston; diamonds, dashed line: creviced piston. Initial pressure  $P_0 = 106.7$  kPa.

Figure 4: Ignition delay times of stoichiometric (diamonds) and  $\Phi = 0.7$  (circles) CH<sub>4</sub>/O<sub>2</sub>/inert mixtures as a function of  $T_C$ . Initial pressure  $P_0 = 106.7$  kPa.

Figure 5: Ignition delay times of stoichiometric NG/O<sub>2</sub>/inert mixtures as a function of  $T_C$ . Initial pressure :  $P_0 = 80$  kPa (triangles),  $P_0 = 93.3$  kPa (circles),  $P_0 = 106.7$  kPa (diamonds).

Figure 6: Ignition delay times of stoichiometric (diamonds) and  $\Phi = 0.7$  (circles) NG/O<sub>2</sub>/inert mixtures as a function of  $T_C$ . Initial pressure  $P_0 = 106.7$  kPa.

Figure 7: Ignition delay times of stoichiometric NG/O<sub>2</sub>/inert (diamonds) and CH<sub>4</sub>/O<sub>2</sub>/inert (circles) mixtures as a function of  $T_C$ . Initial pressure:  $P_0 = 106.7$  kPa.

Figure 8: Ignition delay times of stoichiometric NG/O<sub>2</sub>/inert (diamonds), 80/20 NG/H<sub>2</sub>/O<sub>2</sub>/inert (circles) and 40/60 NG/H<sub>2</sub>/O<sub>2</sub>/inert (triangles) mixtures as a function of  $T_C$ . Initial pressure:  $P_0 = 106.7$  kPa.

Figure 9: Ignition delay times of stoichiometric NG/O<sub>2</sub>/inert (diamonds), 90/10 NG/CO/O<sub>2</sub>/inert (circles), 80/20 NG/CO/O<sub>2</sub>/inert (triangles) and 70/30 NG/CO/O<sub>2</sub>/inert (squares) mixtures as a function of  $T_C$ . Initial pressure:  $P_0 = 106.7$  kPa.

1  
2  
3 Figure 10: Ignition delay times of stoichiometric NG/O<sub>2</sub>/inert (diamonds), 90/10  
4 NG/CO<sub>2</sub>/O<sub>2</sub>/inert (circles), 80/20 NG/CO<sub>2</sub>/O<sub>2</sub>/inert (triangles) and 70/30  
5 NG/CO<sub>2</sub>/O<sub>2</sub>/inert (squares) mixtures as a function of T<sub>C</sub>. Initial pressure: P<sub>0</sub> = 93.3  
6 kPa.  
7  
8  
9

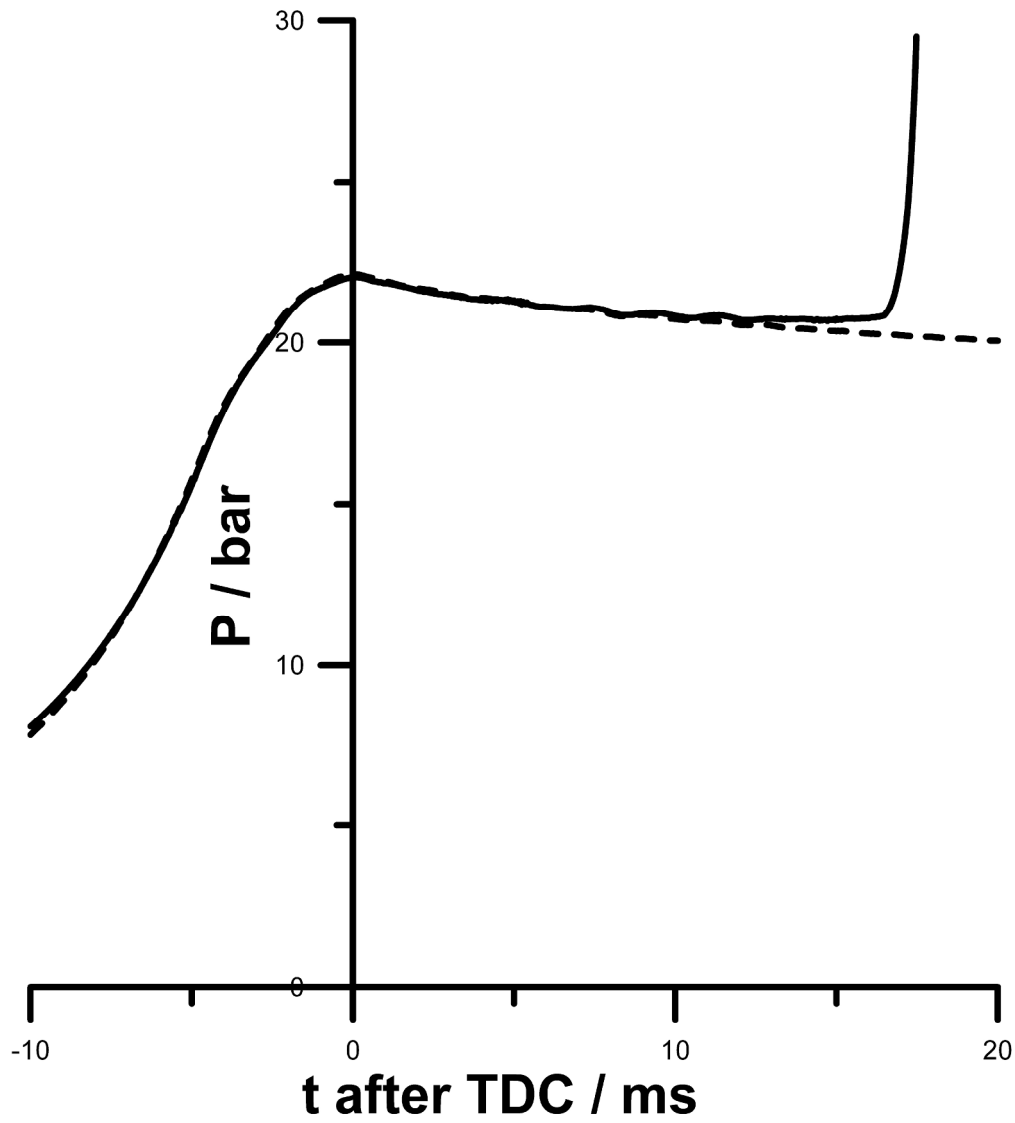
10  
11 Figure 11: Ignition delay times of stoichiometric NG/O<sub>2</sub>/inert (diamonds) and 70/30  
12 NG/H<sub>2</sub>O/O<sub>2</sub>/inert (circles) mixtures as a function of T<sub>C</sub>. Initial pressure: P<sub>0</sub> = 93.3 kPa.  
13

14 Figure 12: Effect of additive blending on the ignition delays of NG/O<sub>2</sub>/inert mixtures.  
15 Hydrogen (diamonds): T<sub>C</sub> = 936 K, CO (circles): T<sub>C</sub> = 917 K, H<sub>2</sub>O (squares): T<sub>C</sub> = 937  
16 K, CO<sub>2</sub> (triangles): T<sub>C</sub> = 920 K.  
17  
18  
19  
20

21  
22 Figure 13: Comparison of the experimental and simulated ignition delays of  
23 stoichiometric NG/O<sub>2</sub>/inert mixtures at three initial pressures: P<sub>0</sub> = 106.7 kPa  
24 (diamonds, thick line), P<sub>0</sub> = 93.3 kPa (circles, medium line), P<sub>0</sub> = 80 kPa (triangles,  
25 thin line). LENI model (long dash), NUIG model (full line), USC model (short dash),  
26 GRI+RAMEC (dash-dot).  
27  
28  
29  
30  
31  
32

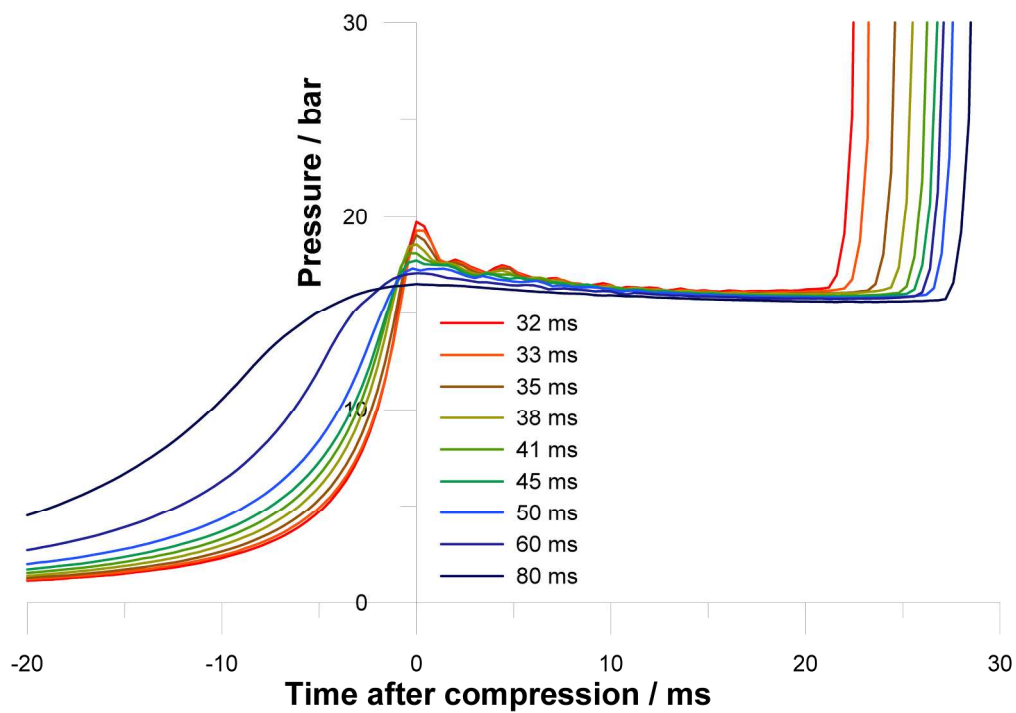
33  
34 Figure 14: Simulated pressure profiles obtained in stoichiometric mixtures at P<sub>0</sub> = 80  
35 kPa and T<sub>0</sub> = 363 K for: NG/O<sub>2</sub>/Ar, with the compression phase (full line), without the  
36 compression phase (crosses). NG/H<sub>2</sub>(40/60)/O<sub>2</sub>/Ar, with the compression phase  
37 (dash-dotted line), without the compression phase (dashed line).  
38  
39  
40  
41  
42

43 Figure 15: Comparison of the experimental and simulated effect of additive blending  
44 on the ignition delays of NG/O<sub>2</sub>/inert mixtures. Simulations are performed with the  
45 NUIG mechanism. Experimental data: see Figure 12. Modelling: H<sub>2</sub> (full line), CO  
46 (long dash), H<sub>2</sub>O (dash-dot), CO<sub>2</sub> (short dash).  
47  
48  
49  
50  
51  
52  
53  
54  
55  
56  
57  
58  
59  
60

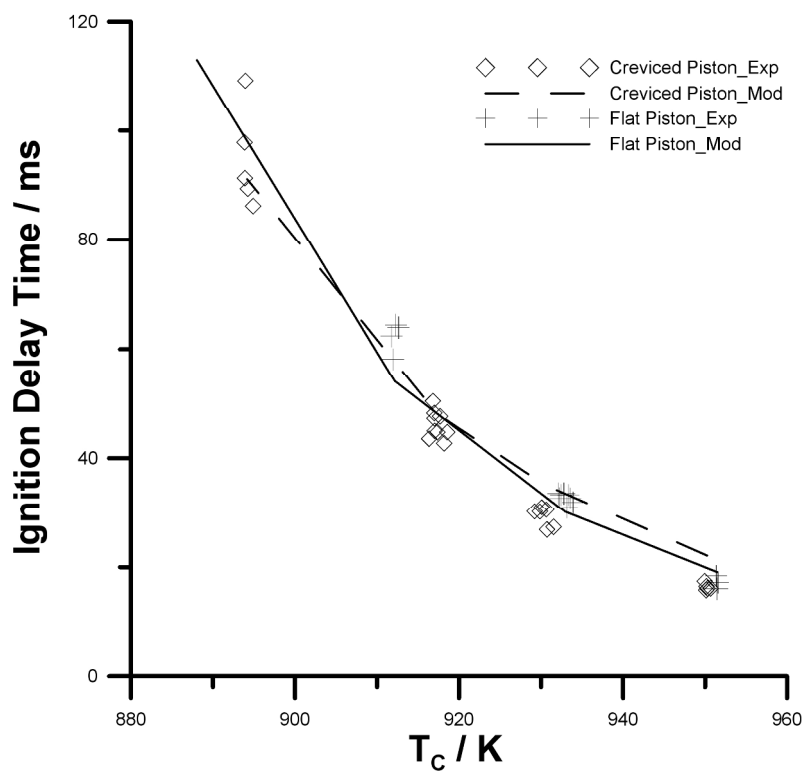


152x170mm (600 x 600 DPI)

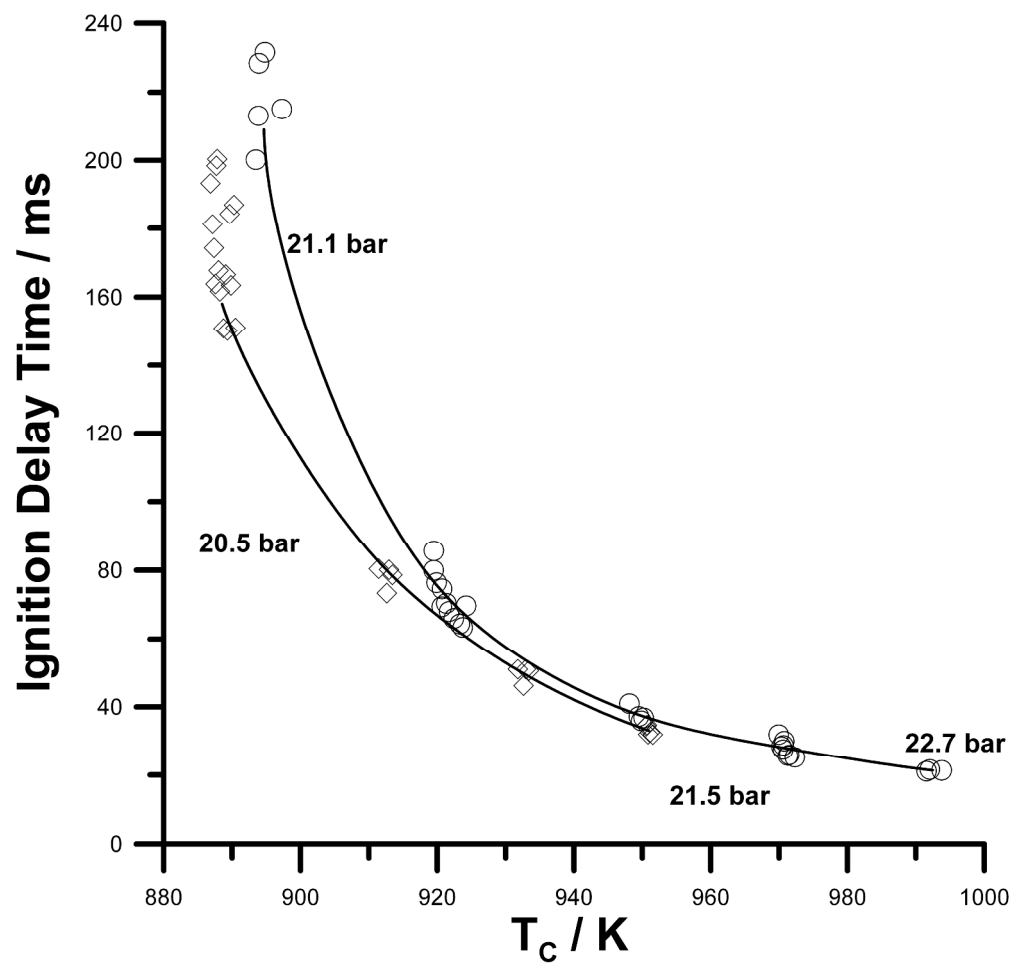
1  
2  
3  
4  
5  
6  
7  
8  
9  
10  
11  
12  
13  
14  
15  
16  
17  
18  
19  
20  
21  
22  
23  
24  
25  
26  
27  
28  
29  
30  
31  
32  
33  
34  
35  
36  
37  
38  
39  
40  
41  
42  
43  
44  
45  
46  
47  
48  
49  
50  
51  
52  
53  
54  
55  
56  
57  
58  
59  
60



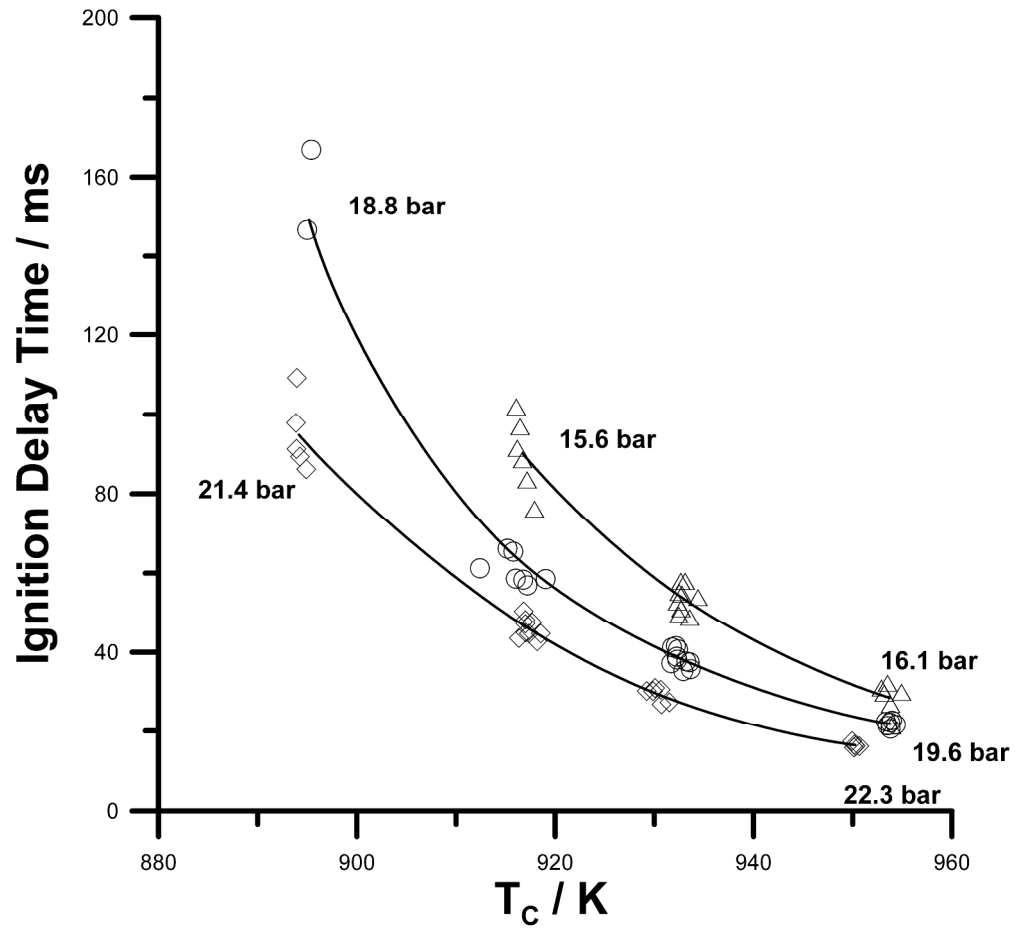
109x76mm (600 x 600 DPI)



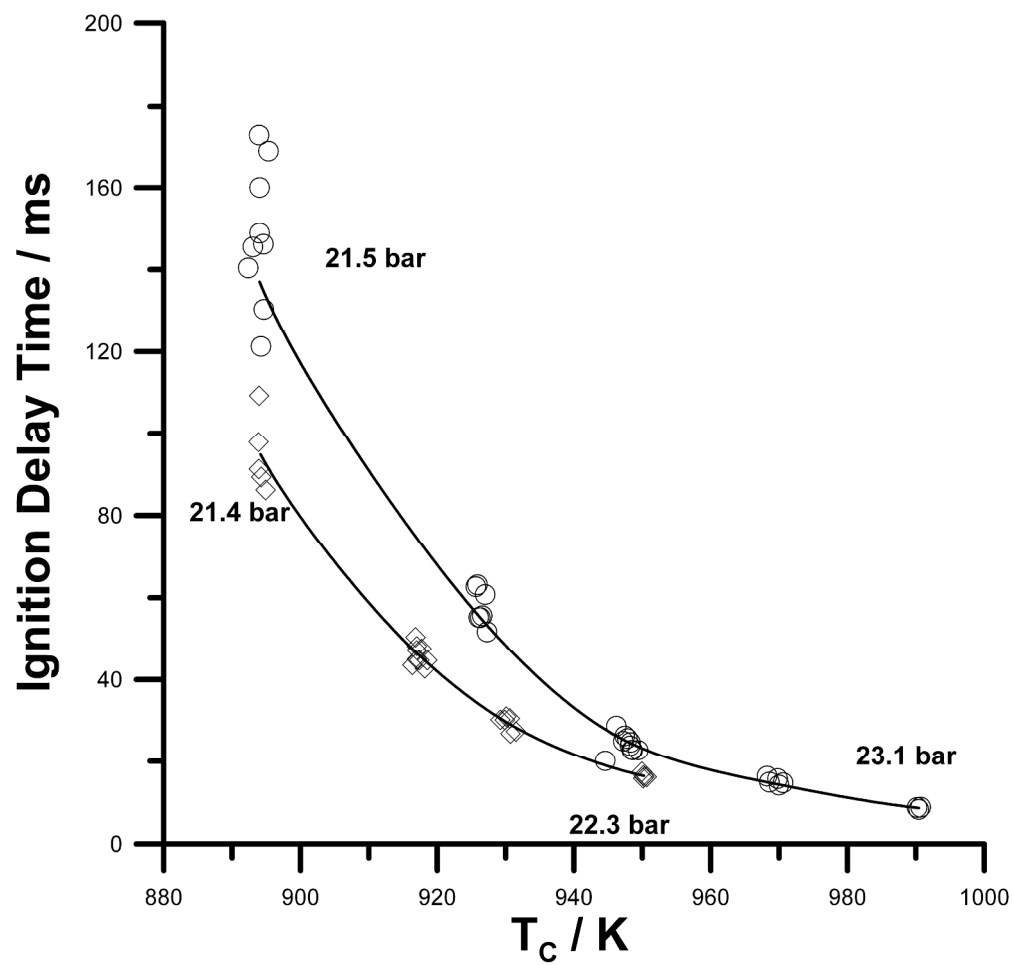
578x872mm (96 x 96 DPI)



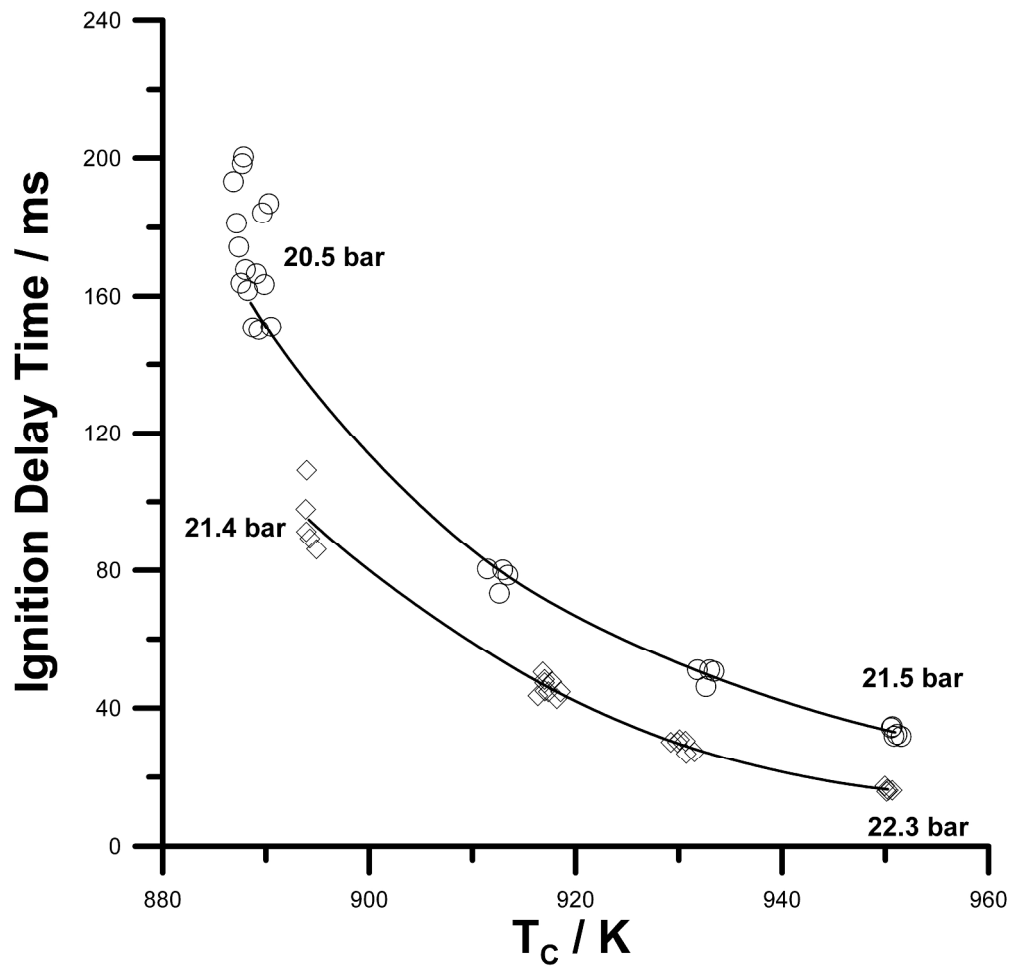
145x139mm (600 x 600 DPI)



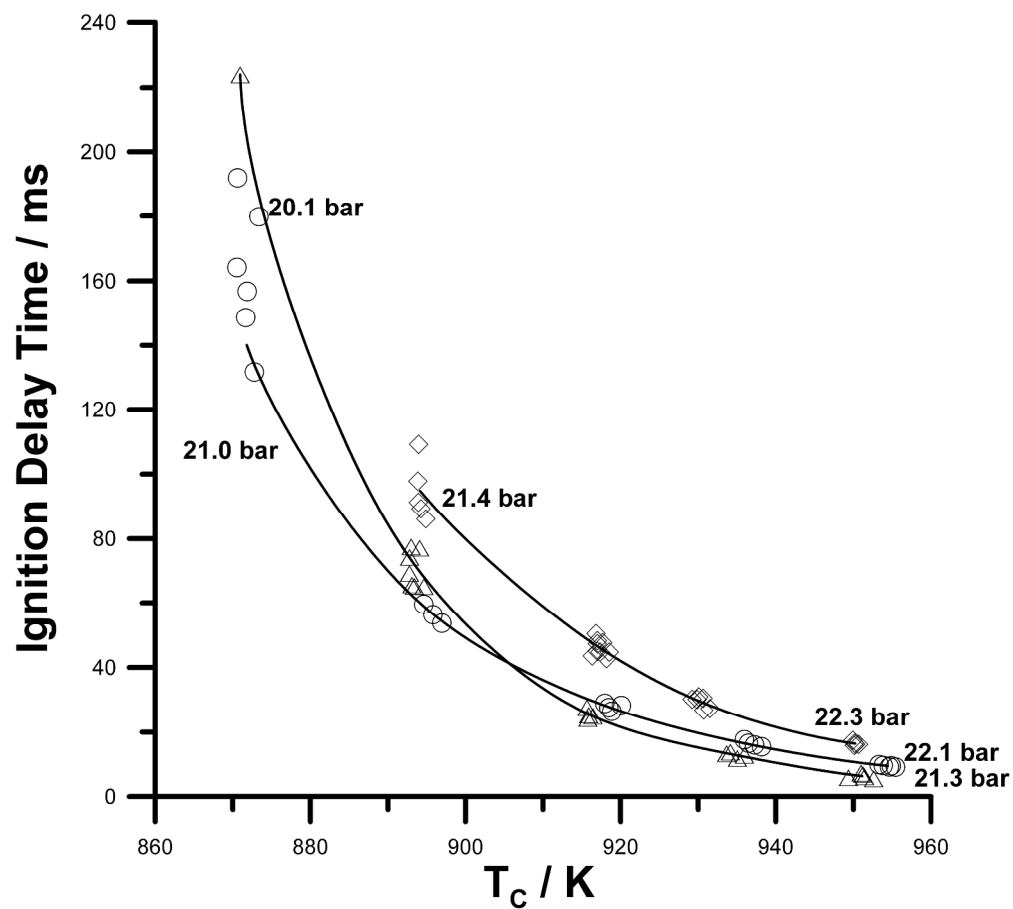
140x130mm (600 x 600 DPI)



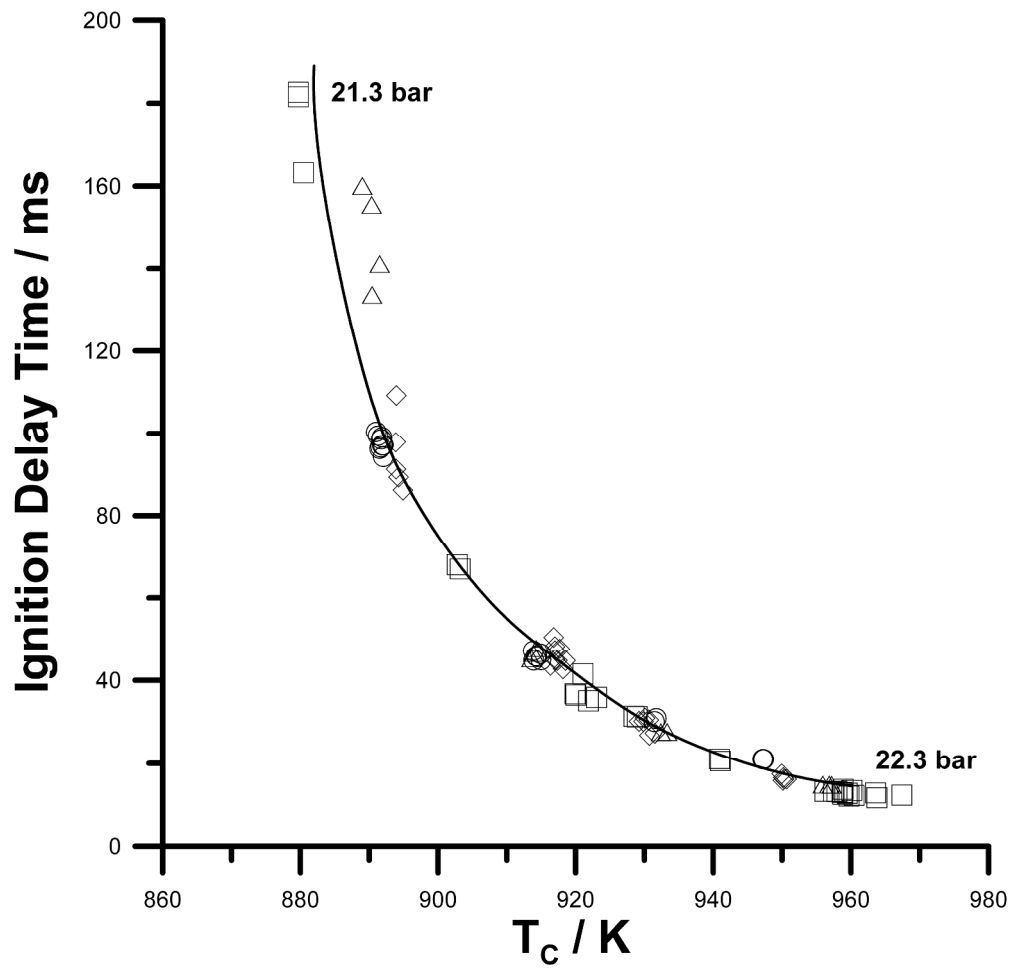
145x139mm (600 x 600 DPI)



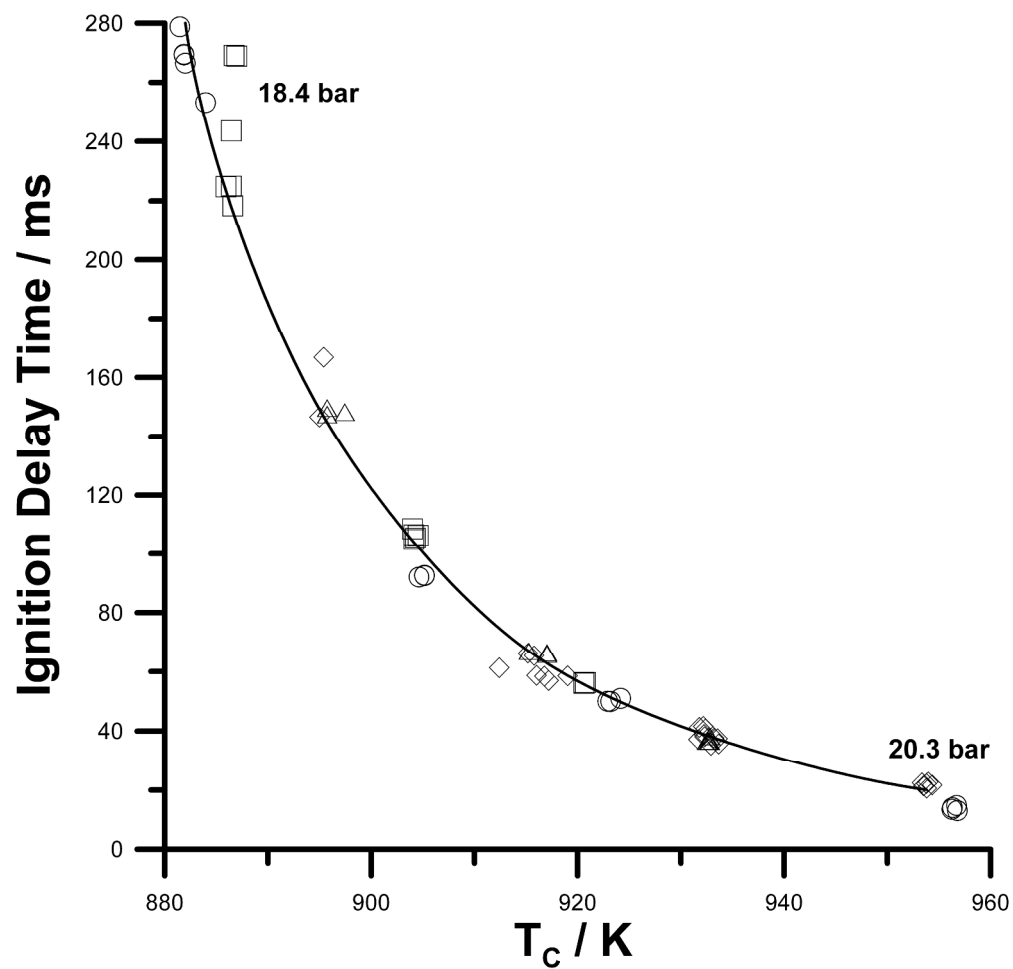
146x140mm (600 x 600 DPI)



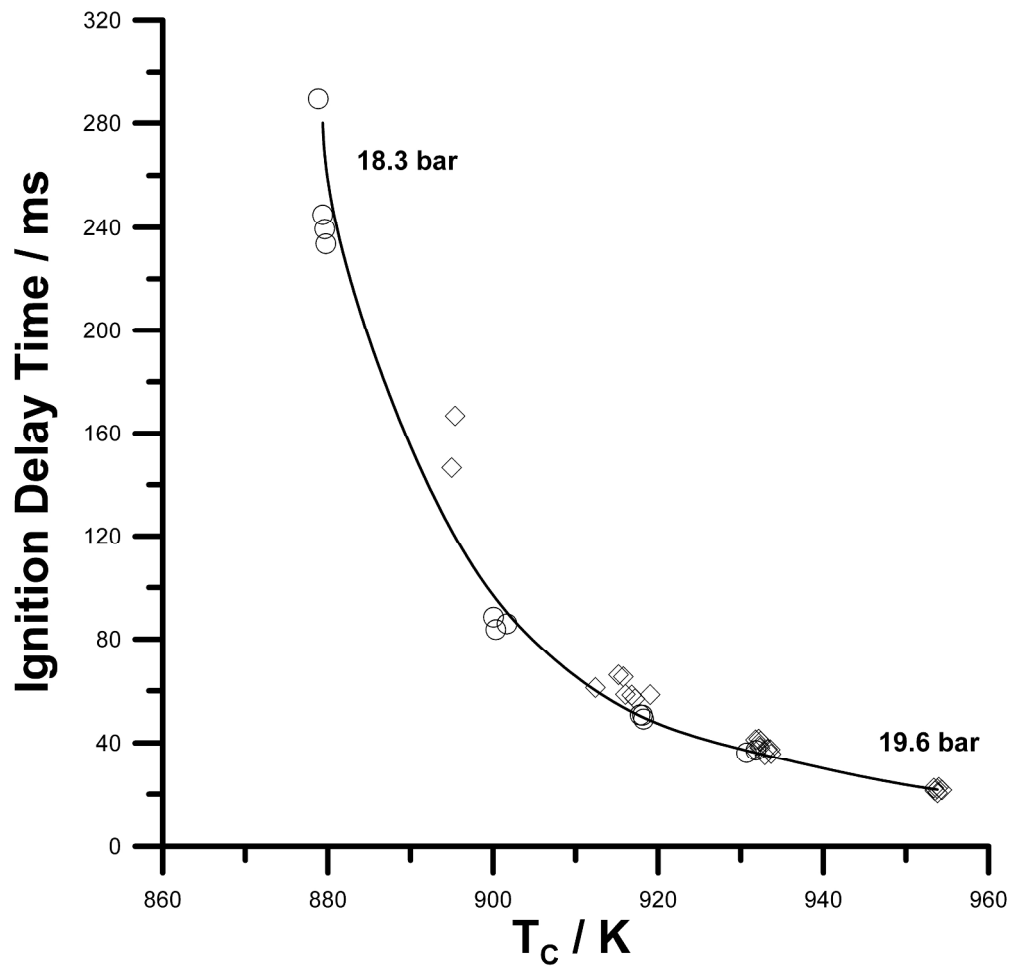
137x124mm (600 x 600 DPI)



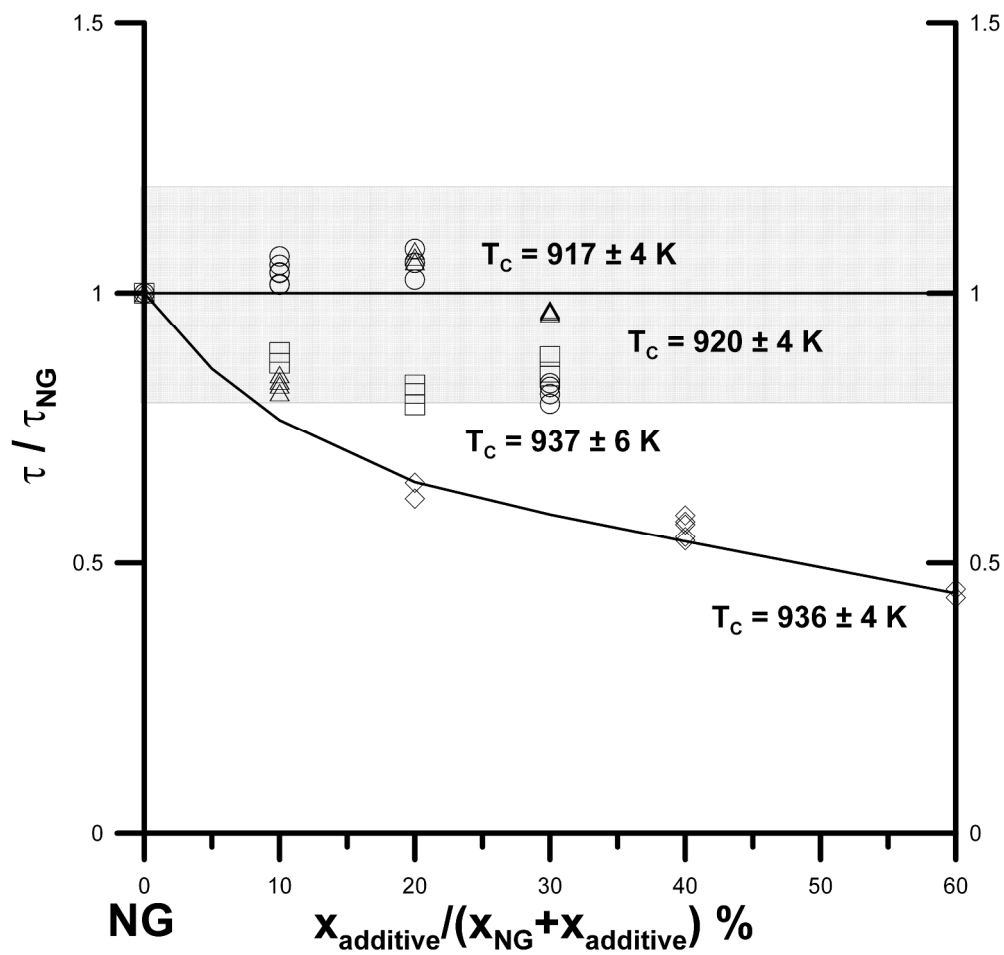
146x140mm (600 x 600 DPI)



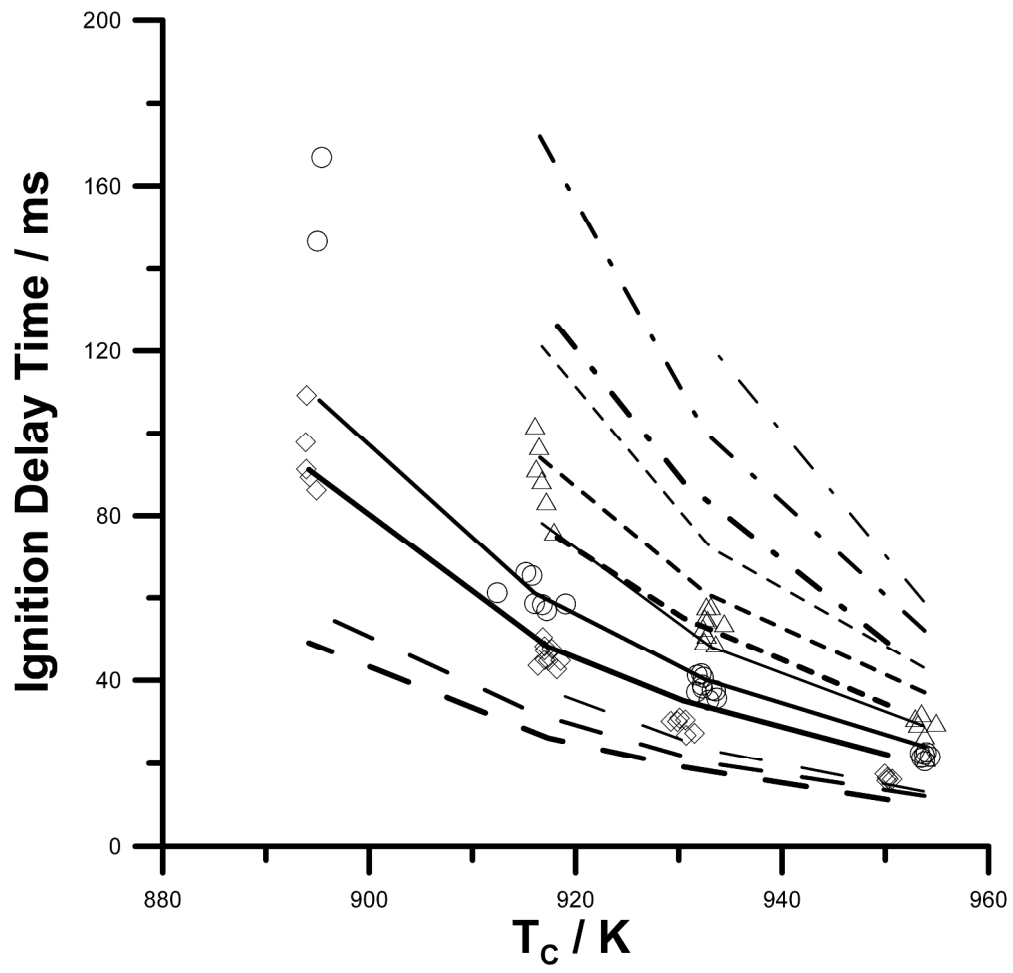
146x140mm (600 x 600 DPI)



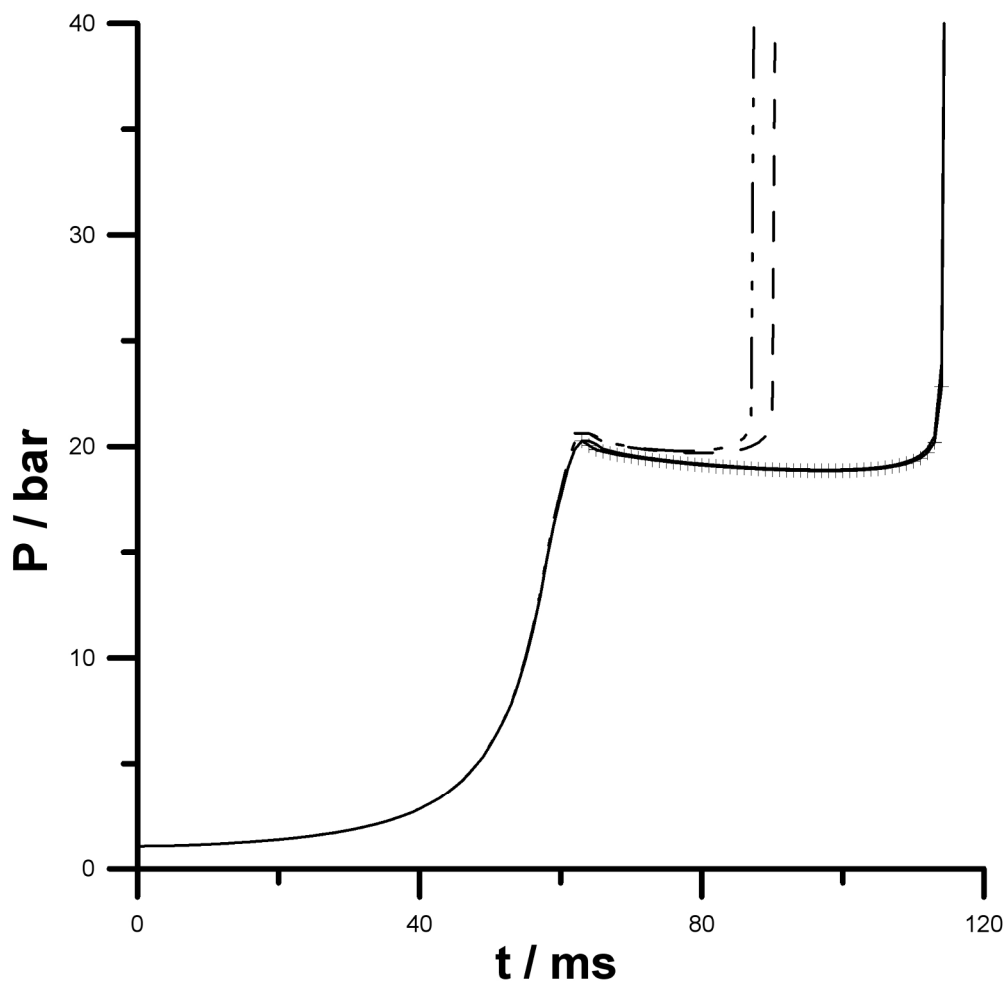
146x140mm (600 x 600 DPI)



143x136mm (600 x 600 DPI)

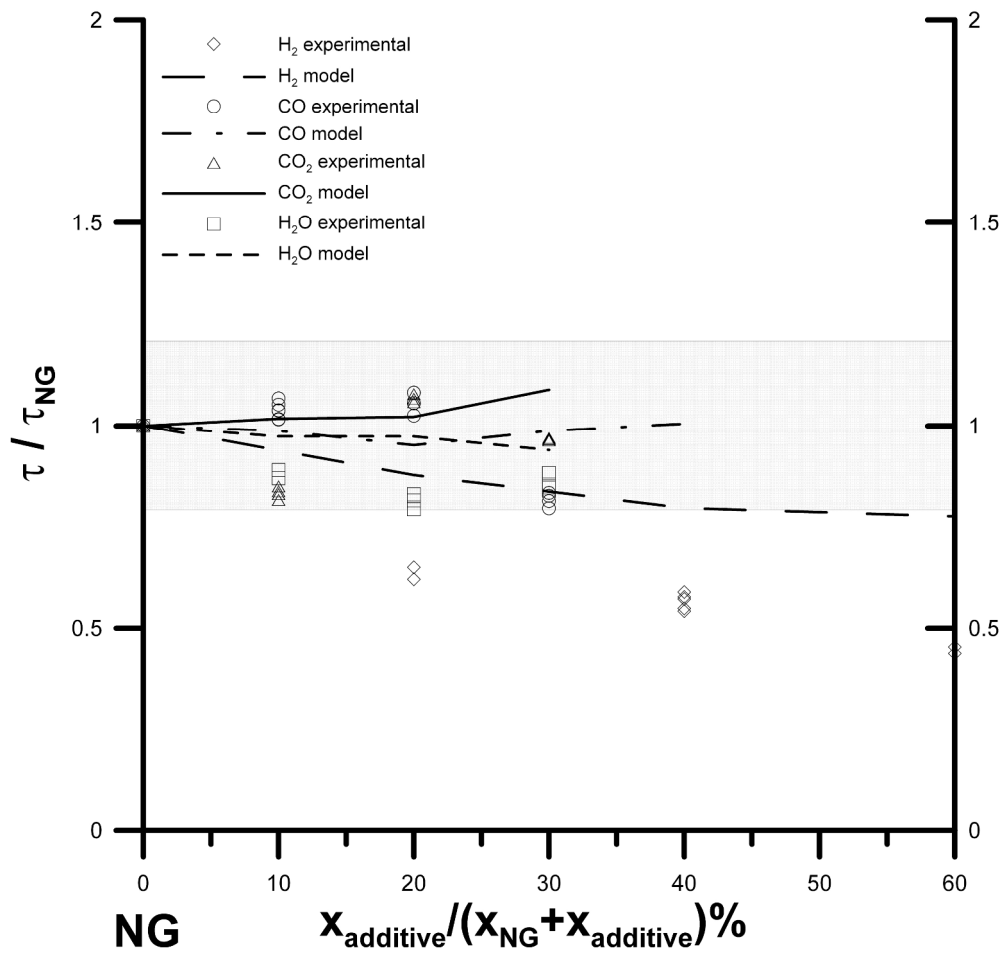


146x140mm (600 x 600 DPI)



562x550mm (96 x 96 DPI)

1  
2  
3  
4  
5  
6  
7  
8  
9  
10  
11  
12  
13  
14  
15  
16  
17  
18  
19  
20  
21  
22  
23  
24  
25  
26  
27  
28  
29  
30  
31  
32  
33  
34  
35  
36  
37  
38  
39  
40  
41  
42  
43  
44  
45  
46  
47  
48  
49  
50  
51  
52  
53  
54  
55  
56  
57  
58  
59  
60



144x137mm (600 x 600 DPI)